A Fixed Grid method for hyperelastic models in large strain analysis using the Level Set Method

William Ramírez Benitez

Manuel J Garcia.

Grupo de Investigación Mecánica Aplicada , universidad EAFIT, Medellín, Colombia

wramirez@eafit.edu.co

March 12, 2014

Abstract

A Fixed Grid Finite Element Method (FGFEM) in addition to a Mooney-Rivlin hyperelastic model is introduced. This method uses the mixed finite element formulation to treat the elements, but classifying these in a fixed cartesian grid that is superimposed over the model geometry. In order to do this, the boundary tracking is achieved by solving the level set equation. A numerical extrapolation of the displacement field from the solid domain to the entire fixed grid domain is done. The system of equations are solved by the use of an incremental Newton-Raphson scheme. Finally, some numerical examples are implemented and good convergence results are obtained for the displacement field, showing that FGFEM for the hyperelastic model is suitable for mechanical problems undergoing large strains and large displacements.

1 Introduction

The Fixed Grid Finite Element Method (FGFEM) was introduced in [2]. This shows to be an efficient and accuracy method to approximate the displacement field in Linear Elastic problems. It is based on a fixed grid representation of the model geometry and had been used successfully in optimization methods as ISO- ESO[8].

The easy representation of the model geometry and the efficient computation of the elements properties are the main advantages of using fixed grid methods. This is why an implementation of a geometric and material nonlinear formulation using this approach may imply an extension of this advantages to a large amount of engineering problems. In this work, the Level Set Method is used in order to track the boundary, which is discontinuous at the element level.

Numerical methods as the eXtended Finite Element Method (X-FEM) may be compared with FGFEM since both treat discontinuities in a similar fashion. In [6] the Level Set Method is coupled to X-FEM in order to model arbitrary holes and material interfaces (inclusions) without meshing the internal boundaries. The disadvantage in this work is that numerical integration of the elements at the interfaces are treated via re-meshing process, which implies more computation costs.

Another example of the use of the Level Set Method in not-matching meshes is contained in [5]. Here, the Level Set Equation is used along with X-FEM in order to model dynamic crack propagation in elastic-plastic media. In this formulation, the degrees of freedom are increased at the element level, which may seen as a drawback of the formulation.

In [3] unstructured meshes are used to model hyperelastic materials. Level Set is employed for topological shape optimization problems using solid isotropic materials with penalization

(SIMP). The main drawback of applying unstructured formulation approaches is that different meshes are used to model the problem geometry and the grid domain. The idea of using a fixed grid is that its same regular elements are used to solve the established problem.

In this work FGFEM in addition to a Mooney-Rivlin hyperelastic model is introduced. The Level Set equation is used in order to track the boundary evolution. Numerical integration over discontinuous elements is efficiently achieved via computation of a weighted average of their areas.

2 The Fixed Grid Finite Element Method (FGFEM)

The Fixed Grid Method Finite Element Method was developed to approximate the displacement field in mechanical linear elastic problems. This superimposes a cartesian grid on the geometry model instead of building a mesh that fits the geometry, as the traditional finite element method. This method classifies the quadrilateral finite elements that are inside the geometry (I), outside the geometry (O) and the elements that are neither inside nor outside (NIO), figure (1) illustrates the method. Generally, the properties of the outside elements are imposed such that these are very small compared with the properties of the inside elements (see [2]). Another way to treat these elements is eliminating the nodes that are outside the geometry and that are not shared with NIO or I elements. There are many different ways in which the NIO elements may be

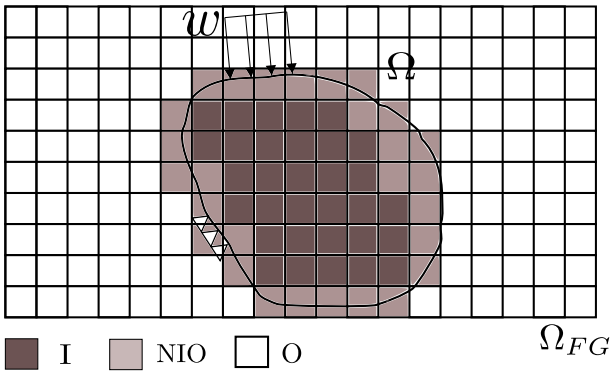

Figure 1: The Fixed Grid Method

computed. The method used in this work is a weighted average of the areas of the element that are inside and outside the geometry. This approximation shows to be suitable for the hyperelastic model.

There are many advantages in using this method. One of these is that the stiffness matrix have to be computed only once for the I elements, making the method computationally efficient.

3 Mooney-Rivlin model for an hyperelastic material

The Mooney-Rivlin material description is used to model incompresible materials (rubber-like materials) undergoing large strains ([7]). The strain energy density for the Mooney-Rivlin model is usually defined as

$$\begin{aligned} {}^t_0\bar{W} &= C_1\left({}^t_0I_1 - 3\right) + C_2\left({}^t_0I_2 - 3\right); \\ {}^t_0I_3 &= 1, \end{aligned} \tag{1}$$

where C_1 and C_2 are material constants and the invariants ${}^t_0I_1$, ${}^t_0I_2$ and ${}^t_0I_3$ are defined as

$${}^t_0I_1 = {}^t_0C_{kk} \tag{2}$$

$${}^t_0I_2 = \frac{1}{2}\left(\left({}^t_0I_1\right)^2 - {}^t_0C_{ij}{}^t_0C_{ij}\right) \tag{3}$$

$$ {}^t_0 I_1 = det\left({}^t_0\mathbf{C}\right), \tag{4} $$

where ${}^t_0\mathbf{C}$ is the right Cauchy-Green deformation tensor. However, this description is frequently modified as follows

$$ {}^t_0\bar{W} = C_1\left({}^t_0 J_1 - 3\right) + C_2\left({}^t_0 J_2 - 3\right) + W_H({}^t_0 J_3), \tag{5} $$

where

$$ {}^t_0 J_1 = {}^t_0 I_1 {}^t_0 I_3^{-1/3} \tag{6} $$

$$ {}^t_0 J_2 = {}^t_0 I_2 {}^t_0 I_3^{-2/3} \tag{7} $$

$$ {}^t_0 J_3 = {}^t_0 I_3^{1/2}, \tag{8} $$

4 Finite element formulation (Displacement/Pressure formulation)

A displacement/pressure (u/p) formulation is generally used to solve problems undergoing large strains in which an incompresible model is used. The displacement-based nonlinear finite element method is not usually effective. In this work, a Total Lagrangian formulation is used such that all the variables are measured with respect to a reference configuration t.

The system of equations for an hyperelastic problem, using the u/p formulation has the form

$$ \begin{pmatrix} {}^{\mathbf{t}}\mathbf{KUU} & {}^{\mathbf{t}}\mathbf{KUP} \\ {}^{\mathbf{t}}\mathbf{KPU} & {}^{\mathbf{t}}\mathbf{KPP} \end{pmatrix} \begin{pmatrix} \hat{\mathbf{u}} \\ \hat{\mathbf{p}} \end{pmatrix} = \begin{pmatrix} {}^{\mathbf{t+\Delta t}}\mathbf{R} \\ \mathbf{0} \end{pmatrix} - \begin{pmatrix} {}^{\mathbf{t}}\mathbf{FU} \\ {}^{\mathbf{t}}\mathbf{FP} \end{pmatrix}. \tag{9} $$

This system of equations are solved by use of an incremental formulation. Here $\hat{\mathbf{u}}$ and $\hat{\mathbf{p}}$ are the vectors of nodal point incremental displacements and pressures, respectively. ${}^{t+\Delta t}\mathbf{R}$ is the vector of externally applied nodal point loads corresponding to time $t + \Delta t$; and $\mathbf{F} = \left[{}^t\mathbf{FU}, {}^t\,\mathbf{FP}\right]^T$ is the vector of nodal point forces corresponding to the internal element stresses at time t. Due to this, the subtraction at the right hand side is known as the out-of-balance force vector and may reach an small value at the end of each load increment. Generally, this value is established as a percentage of the first out-of-balance vector magnitude at a load increment.

Although the discrete time increment Δt is used, we used it to denote a load increment. Furthermore

$$ FU_i = \int_{{}_0V} {}^t_0 S_{ki} \frac{\partial^t_0 \epsilon_{ki}}{\partial^t \hat{u}_i} d^0V \tag{10} $$

$$ FP_i = \int_{{}_0V} \frac{1}{\kappa}({}^t\bar{p} - {}^t\tilde{p}) \frac{\partial^t \tilde{p}}{\partial^t \hat{p}_i} d^0V \tag{11} $$

$$ KUU_{ij} = \int_{{}_0V} {}_0CUU_{kirs} \frac{\partial^t_0 \epsilon_{ki}}{\partial^t \hat{u}_i} \frac{\partial^t_0 \epsilon_{rs}}{\partial^t \hat{u}_j} d^0V + \int_{{}_0V} {}^t_0 S_{kl} \frac{\partial^{2t}_0 \epsilon_{kl}}{\partial^t \hat{u}_i \partial^t \hat{u}_j} d^0V \tag{12} $$

$$ KUP_{ij} = \int_{{}_0V} {}_0CUP_{ki} \frac{\partial^t_0 \epsilon_{ki}}{\partial^t \hat{u}_i} \frac{\partial^t \tilde{p}}{\partial^t \hat{p}_j} d^0V \tag{13} $$

$$ KPP_{ij} = \int_{{}_0V} -\frac{1}{\kappa} \frac{\partial^t \tilde{p}}{\partial^t \hat{p}_i} \frac{\partial^t \bar{p}}{\partial^t \hat{p}_j} d^0V \tag{14} $$

where

$$ {}^t_0 S_{ki} = {}^t_0 \bar{S}_{ki} - \frac{1}{\kappa}({}^t\bar{p} - {}^t\tilde{p}) \frac{\partial^t \bar{p}}{\partial^t_0 \epsilon_{ki}} \tag{15} $$

$$ {}_0CUU_{kirs} = {}_0\bar{C}_{kirs} - \frac{1}{\kappa} \frac{\partial^t \bar{p}}{\partial^t_0 \epsilon_{ki}} \frac{\partial^t \bar{p}}{\partial^t_0 \epsilon_{rs}} - \frac{1}{\kappa}({}^t\bar{p} - {}^t\tilde{p}) \frac{\partial^{2t} \bar{p}}{\partial^t_0 \epsilon_{rs} \partial^t_0 \epsilon_{ki}} \tag{16} $$

$$ {}_0CUP_{ki} = \frac{1}{\kappa} \frac{\partial^t \bar{p}}{\partial^t_0 \epsilon_{ki}}. \tag{17} $$

The second Piola-Kirchhoff stress tensor is defined in terms of the strain energy density as follows

$$ {}^{t}_{0}S_{kl} = \frac{1}{2}\left(\frac{\partial^t_0 \bar{W}}{\partial^t_0 \epsilon_{kl}} + \frac{\partial^t_0 \bar{W}}{\partial^t_0 \epsilon_{lk}}\right), \tag{18} $$

for the constitutive tensor we have

$$ {}^{t}_{0}C_{klrs} = \frac{1}{2}\left(\frac{\partial^t_0 \bar{S}_{kl}}{\partial^t_0 \epsilon_{rs}} + \frac{\partial^t_0 \bar{S}_{kl}}{\partial^t_0 \epsilon_{sr}}\right) \tag{19} $$

4.1 Static condensation

As the pressure increments are discontinuous betwen elements, is more efficient to condense out this variable ([7]). Using equation (9), it can be shown that

$$ \hat{\mathbf{p}} = \mathbf{KPP}^{-1}\left(-\mathbf{FP} - \mathbf{KUP}^T\hat{\mathbf{u}}\right) \tag{20} $$

Now, the system of equations can be solved in terms of the displacement increments

$$ \mathbf{K}\hat{\mathbf{u}} = \mathbf{R} - \mathbf{F}, \tag{21} $$

where

$$ \mathbf{K} = \mathbf{KUU} - \mathbf{KUPKPP}^{-1}\mathbf{KUP}^T \tag{22} $$

$$ \mathbf{F} = \mathbf{FU} - \mathbf{KUPKPP}^{-1}\mathbf{FP} \tag{23} $$

5 Fixed Grid Method for the hyperelastic model

In the previous section the finite element formulation for an element using a mixed formulation was done. In this section the formulation for the Fixed Grid Method is performed using these results.

The main idea of the FGFEM in linear elastic problems is to work with a cartesian grid and classify the elements as I, O and NIO. For the hyperelastic problem the formulation may be implemented in a similar fashion.

Properties of the O elements in the linear elastic problem are multiplied by a small factor. In the hyperelastic problem this leads to an ill-conditioned stiffness matrix and the problem can not be solved. Therefore, the degress of freedom which are outside the model geometry are eliminated as it is done for the dirichlet boundary conditions.

I elements are treated using the formulation that was introduced in the previos section. for the NIO elements the matrices in equation (9) are modified as follows

$$ \mathbf{FU} = (\xi)\mathbf{FU}_0 \tag{24} $$

$$ \mathbf{FP} = (\xi)\mathbf{FP}_0 \tag{25} $$

$$ \mathbf{KUU} = (\xi)\mathbf{KUU}_0 \tag{26} $$

$$ \mathbf{KUP} = (\xi)\mathbf{KUP}_0 \tag{27} $$

$$ \mathbf{KPP} = (\xi)\mathbf{KPP}_0 \tag{28} $$

where the 0 subscript indicates the matrices computed using the u/p formulation for an I element. These are premultiplied by a ξ factor which is computed as

$$ \xi = A_{inside}/A \tag{29} $$

where A_{inside} is the area of the NIO element that is inside the geometry and A indicates the total area of the element, figure (2) illustrates this. The advantage of using this implementation is that the area fraction ξ has to be computed only once for each NIO element.

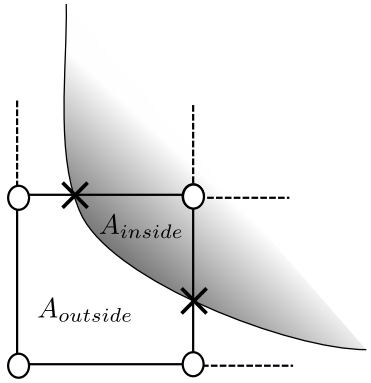

Figure 2: NIO element interception with the model (gray area). White dots represent the element nodes and "X" dots represent the element interception with the model boundary.

6 Tracking the boundary. Level Set Method

The Level Set Method is a method to represent a moving boundary implicitly. It is based on an implicit function $R^d \ni [\mathbf{x}, t] \mapsto \phi(\mathbf{x}, t)$ that is defined as follows, let $\Omega \subset R^d$ a bounded domain and D a rectangular bounded domain enclosing Ω:

$$\phi = \begin{cases} \phi(\mathbf{x}, t) > 0 & \forall \mathbf{x} \in \Omega \setminus \partial\Omega \\ \phi(\mathbf{x}, t) = 0 & \forall \mathbf{x} \in \partial\Omega \\ \phi(\mathbf{x}, t) < 0 & \forall \mathbf{x} \in D \setminus \Omega \end{cases} \tag{30}$$

The evolution of the implicit boundary $\partial\Omega$ can be traced finding the solution of the advection equation:

$$\frac{\partial \phi(\mathbf{x}, t)}{\partial t} + \vec{\mathbf{v}} \cdot \nabla\phi = 0, \tag{31}$$

$$\phi(\partial\mathbf{x}, 0) = \phi_0(\mathbf{x}) \tag{32}$$

where $\vec{\mathbf{v}}$ is the velocity field of the boundary.

In order to adapt this method to the FGFEM hyperelastic formulation (i. e. only the displacement is known) this velocity is replaced by the computed displacement field $\vec{\mathbf{u}}$, using an estimated time t. Accordingly, the Level Set Equation is modified as follows

$$\frac{\partial \phi(\mathbf{x}, t)}{\partial t} + \frac{\vec{\mathbf{u}}}{t} \cdot \nabla\phi = 0. \tag{33}$$

This equation is solved using finite differences, employing an upwind approach.

In order to satisfy the Courant-Friedrichs-Lewy (CFL) condition, the time step is calculated as follows

$$\frac{\Delta t}{t} \left(\frac{max\left\{\vec{\mathbf{u}}\right\}}{min\left\{\Delta x, \Delta y\right\}} \right) = \alpha, \tag{34}$$

a common conservative choice is set $\alpha = 0.5$.

A signed distance function is used to represent the implicit boundary. Frequently, this is defined as follows:

$$\phi = \begin{cases} d(\mathbf{x}, \partial\Omega) & \forall \mathbf{x} \in \Omega \setminus \partial\Omega \\ 0 & \forall \mathbf{x} \in \partial\Omega \\ -d(\mathbf{x}, \partial\Omega) & \forall \mathbf{x} \in D \setminus \Omega \end{cases} \tag{35}$$

where $d(., \partial\Omega)$ denotes the usual Euclidean distance function to the set $\partial\Omega$. The signed distance function has the property that

$$\|\nabla\phi\| = 1, \tag{36}$$

which is very advantageous since the level set equation may be computed efficiently.

7 Displacement extrapolation

One problem of using a level equation to tracking the boundary is that the displacement is known only inside and on the interface of the model geometry. The displacement field have to be known over the entire cartesian grid in order to solve the advection equation ([4]). A technique which is is used to propagate the displacement information outward the boundary is using the following equation

$$S_t + \vec{\mathbf{n}} \cdot \nabla S = 0 \tag{37}$$

the normal $\vec{\mathbf{n}}$ in this equation is usually computed using the Signed Distance Function and upwind differencing for each component of the displacement field. It is also known that fields of this type have a tendency to preserve signed distance functions.

The full non-linear finite element method using level set presented here is described in table (1) below. In this pseudo-code the **Kintegral**() sub-routine is used to calculate the matrices presented in equations (10) through (14). Basically, this sub-routine depends on the material properties, pressure and displacement increments to control the geometric and material non-linearities. Having calculated these matrices, an static condensation is executed in order to know the new displacement increment, which is computed using the Newthon-Raphson scheme. Pressure increments are determined in the same fashion.

The **DisplExtra**() sub-routine uses the initial implicit function ϕ_{ini} to extrapolate the displacements calculated in the non-linear FEM scheme to the entire fixed grid domain. Once the displacements over the whole fixed grid domain are known, the **LevelSet**() sub-routine is called in order to compute the level set equation.

The **SignedDistanceF**() sub-routine at the beginning of the algorithm handles the signed distance function calculation. A brute force strategy is used to compute this function. This is not a problem in not-changing two dimensional grids. More efficiently schemes may be encountered in [9] and [1].

8 Numerical examples

In this section some numerical examples are developed to show some results of the Fixed Grid Method using an hyperelastic model. These are selected in order to get physically representative displacements where the finite elements are highly distorted.

8.1 Rectangle with a hole

This problems is shown in figure (4). A Mooney-Rivlin hyperelastic model is used with $C_1 = 0.6X10^6 Mpa$, $C_2 = 0.3X10^6 Mpa$ and $\kappa = 2000X10^6 Mpa$. A distributed force of $w = 46000N/m$ is applied over line $\bar{GH}$. The problem statement is illustrated in figure (3).

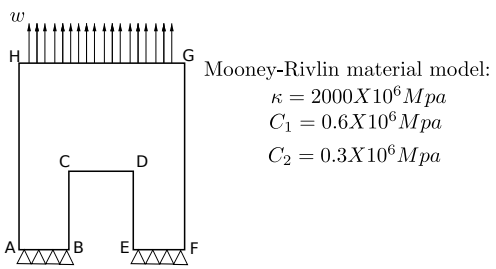

Figure 3: Problem statement. Rectangle with a hole

In figure (4) the initial and final configuration of the Signed Distance Function is showed. A 40X40 grid is used to solve the problem. It has to be pointed that for the out nodes the displacement field can not be computed. Therefore, this information have to be extrapolated using equation (37) at the initial configuration. The pressure is also showed using the initial,

Algorithm 1 pseudo-code of the non-linear fixed grid method with level set tracking

read $Niter$,$nForceIncrem$,$ErroTol$,$LSTime$
Call **SignedDistanceF**(Ω_{FG},Ω_S)
Return ϕ_{ini}
for $j = 1$ **to** $NforceIncrem$ **do**
  Set ${}^{j}\Delta\mathbf{u}_0 \leftarrow 0$
  Set ${}^{j}\Delta\mathbf{p}_0 \leftarrow 0$
  Set $tol \leftarrow BigNumber$
  while $iter \leq Niter$ **and** $error \geq tol$ **do**
    u/p FEM matrices (equ.(10) through (14)) are calculated and numerical integration is done:
    Call **Kintegral** $\left(\kappa, C1, C2, {}^{j+1}\Delta\tilde{p}_{i-1}, {}^{j+1}\Delta\mathbf{u}_{i-1}\right)$
    Return ${}^{j+1}\mathbf{KPP}_i$, ${}^{j+1}\mathbf{KUP}_i$, ${}^{t+\Delta t}\mathbf{FP}_i$, ${}^{j+1}\mathbf{KUU}_{i-1}$ and ${}^{j+1}\mathbf{FP}_{i-1}$
    Static condensation (equ. 22):
    Set ${}^{j+1}\mathbf{K}_{i-1} \leftarrow {}^{j+1}\mathbf{KUU}_{i-1} - {}^{t+\Delta t}\mathbf{KUP}_{i-1}{}^{j+1}\mathbf{KPP}_{i-1}^{-1}{}^{j+1}\mathbf{KUP}_{i-1}^{T}$
    Residual calculation:
    Set ${}^{j+1}\mathbf{R}_{i-1} \leftarrow {}^{j+1}\mathbf{F}^{ext} - {}^{t+\Delta t}\mathbf{F}_{i-1}^{int}$
    Correction over the displacements (Newthon-Raphson scheme):
    Solve ${}^{j+1}\mathbf{K}_{i-1}\mathbf{Cu}_i = {}^{j+1}\mathbf{R}_{i-1}$
    Displacement increments:
    Set ${}^{j+1}\Delta\mathbf{u}_i \leftarrow {}^{t+\Delta t}\Delta\mathbf{u}_{i-1} + \mathbf{Cu}_i$
    Set ${}^{j+1}\mathbf{u}_i \leftarrow {}^{j+1}\mathbf{u}_{i-1} + {}^{t+\Delta t}\Delta\mathbf{u}_i$
    Pressure calculation (equ. 20):
    Set $\mathbf{Cp}_i \leftarrow {}^{j+1}\mathbf{KPP}_{i-1}^{-1}\left(-{}^{j+1}\mathbf{FP}_{i-1} - {}^{j+1}\mathbf{KUP}_{i-1}^{T}\mathbf{Cu}_i\right)$
    Pressure increments:
    Set ${}^{j+1}\Delta\tilde{\mathbf{p}}_i \leftarrow {}^{t+\Delta t}\Delta\tilde{\mathbf{p}}_{i-1} + \mathbf{Cp}_i$
    Set ${}^{j+1}\tilde{\mathbf{p}}_i \leftarrow {}^{j+1}\tilde{\mathbf{p}}_{i-1} + {}^{j+1}\Delta\tilde{\mathbf{p}}_i$
    Error estimation:
    Set $error \leftarrow \|{}^{j+1}\mathbf{R}_{i-1}\|_2$
    Set $tol \leftarrow ErroTol * \|{}^{j+1}\mathbf{R}_0\|_2$
  end while
end for
Displacement extrapolation:
Call **DisplExtra**($\phi_{ini}, \mathbf{u}_{\Omega_S}$)
Return $\mathbf{u}_{\Omega_{FG}}$
Level set tracking:
Call **LevelSet**($LSTime, \phi_{ini}, \mathbf{u}_{\Omega_{FG}}$)
Return ϕ_{final}

or reference, configuration since extrapolation for the pressure at the final configuration is not available yet.

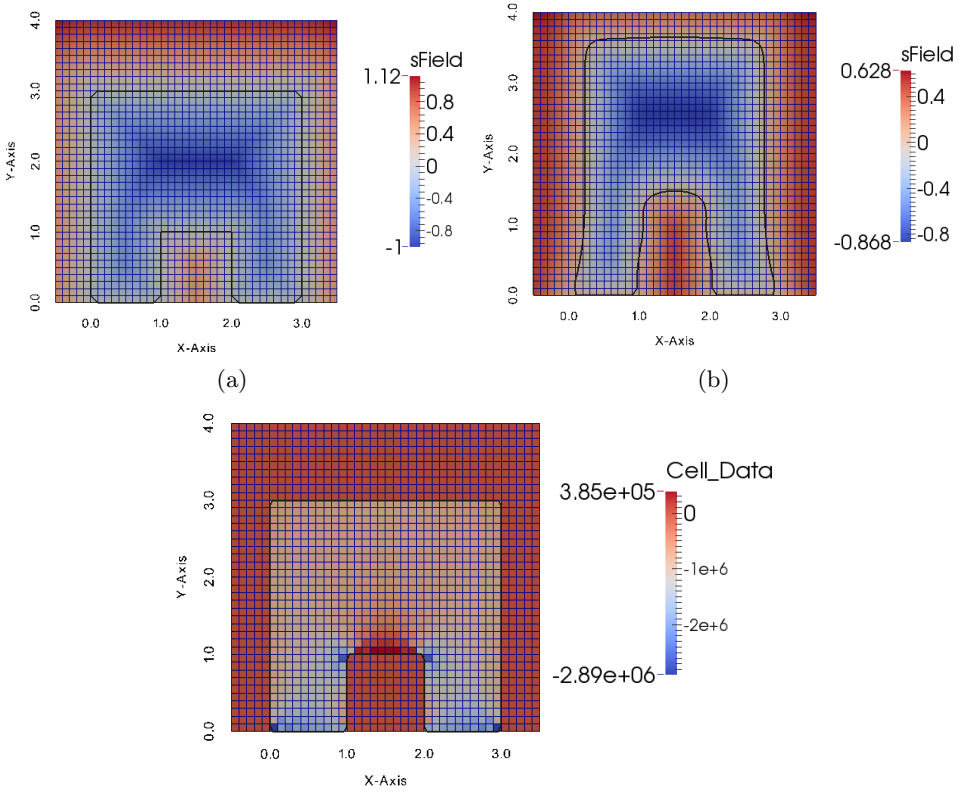

Figure 4: Rectangle with a hole. (a) initial configuration, (b) deformed configuration, (c) pressure

Figure (5) shows the out-of-balance vector magnitude for a load increment. The Euclidean norm is used to determine the residual. For this problem 10 force increments are used to solve the system of equations and a tolerance of 5 % of the first residual is used at each iteration. It can be seen that convergence is achieved at the fourth increment.

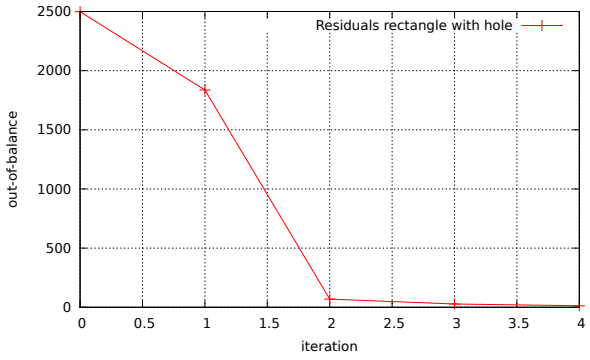

Figure 5: Numerical example, rectagle. Force residual for one increment

8.2 Loaded hyperelastic beam

In this section a loaded hyperelastic beam is taking as an example. The beam is loaded with a distributed force $w = \{100, 10\}\, N/m$ at its top face. A Mooney-Rivlin hyperelastic model is

used with $C_1 = 0.6X10^6 Mpa$, $C_2 = 0.3X10^6 Mpa$ and $\kappa = 2000X10^6 Mpa$. In figure (6) we illustrated the problem statement

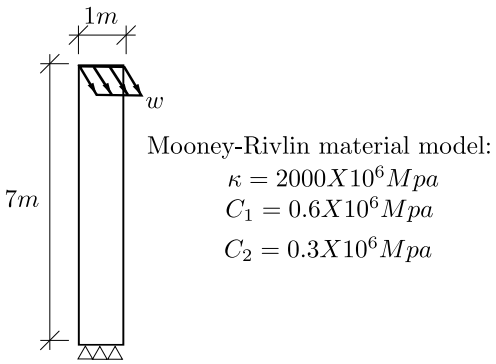

Figure 6: Problem statement. Hyperelastic beam

In figure (7) the initial and final configuration of the Signed Distance Function is showed. A 45X17 grid is used to solve this problem. It has to be notice that a suitable choice of the fixed grid domain has to be done depending of the displacement field. In this particular problem an increment in the load may cause that the model goes beyond the domain as is illustrated in figure (9). However, the Signed Distance Function is still conserved. The pressure is also showed using the initial, or reference, configuration since extrapolation for the pressure at the final configuration is not available yet. Whoever, this pressure seems to be physically consistent since the tension and compression regions may be easily discriminated.

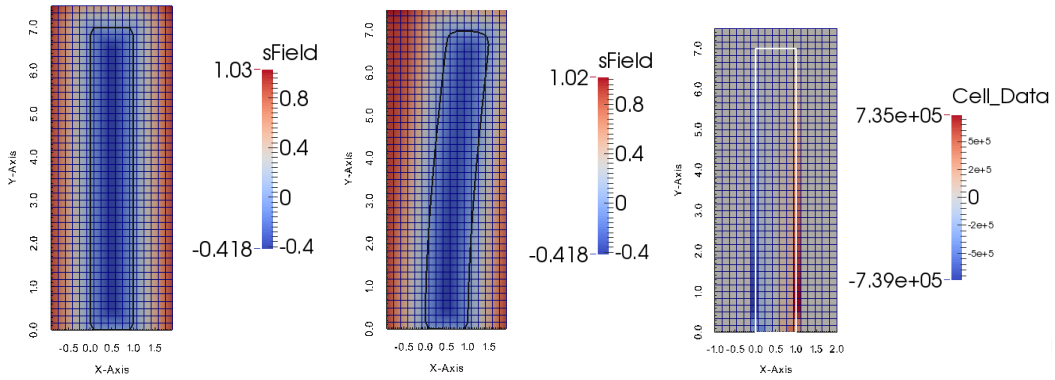

(a) (b) (c)

Figure 7: Hyperelastic beam. (a) initial configuration, (b) deformed configuration, (c) pressure

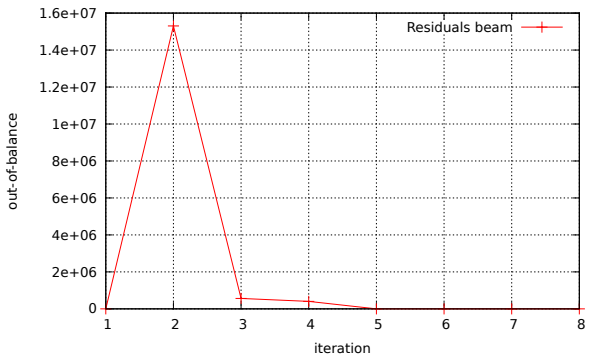

Figure 8: Hyperelastic beam. Out-of-balance vector magnitude for one load increment

Figure (8) shows the out-of-balance vector magnitude for a load increment. The Euclidean

norm is used to determine the residual. As in the previous problem, 10 force increments are used to solve the system of equations. A tolerance of 5 % of the first residual is used at each iteration. In this example, convergence is achieved at the eighth increment.

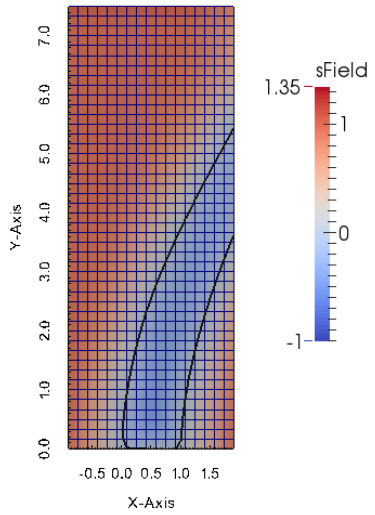

Figure 9: Example of an inadequate Fixed Grid domain

8.3 Loaded hollow square

In this section a loaded hyperelastic square with a hole is taking as an example. The square is loaded with a distributed force $w = -25000N/m$ at its top face. A Mooney-Rivlin hyperelastic model is used with $C_1 = 0.6X10^6Mpa$, $C_2 = 0.3X10^6Mpa$ and $\kappa = 2000X10^6Mpa$. In figure (10) we illustrated the problem statement

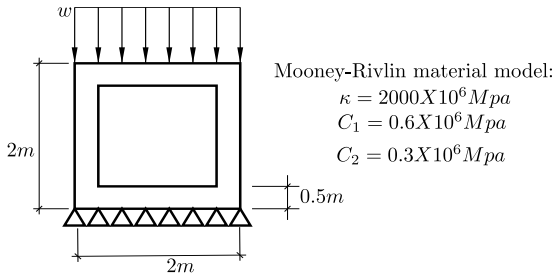

Figure 10: Problem statement. Hollow square

In figure (11) the initial and final configuration of the Signed Distance Function is showed. A 52X45 grid is used to solve this problem. It has to be observed that the load does not depend of the model configuration. Therefore, this is constant during the whole displacement increments. A different configuration may be achieved if a displacemente-dependent load is implemented. The pressure is also showed using the initial, or reference, configuration since extrapolation for the pressure at the final configuration is not available yet.

Figure (12) shows the out-of-balance vector magnitude for a load increment. The Euclidean norm is used to determine the residual. As in the previous problem, 10 force increments are used to solve the system of equations. A tolerance of 5 % of the first residual is used at each iteration. In this example, convergence is achieved at the fourth increment.

It has to be notice that in the last two examples a hight value is reached in the second iteration, which is not the case in the first problem. Therefore, it may be concluded that residuals behaviour could depend on a suitable choice of the problem. As an example, if the material constants are changed, the problem could not converge easily and some parameters, as the load increments, have to be changed in order to achieve good convergence.

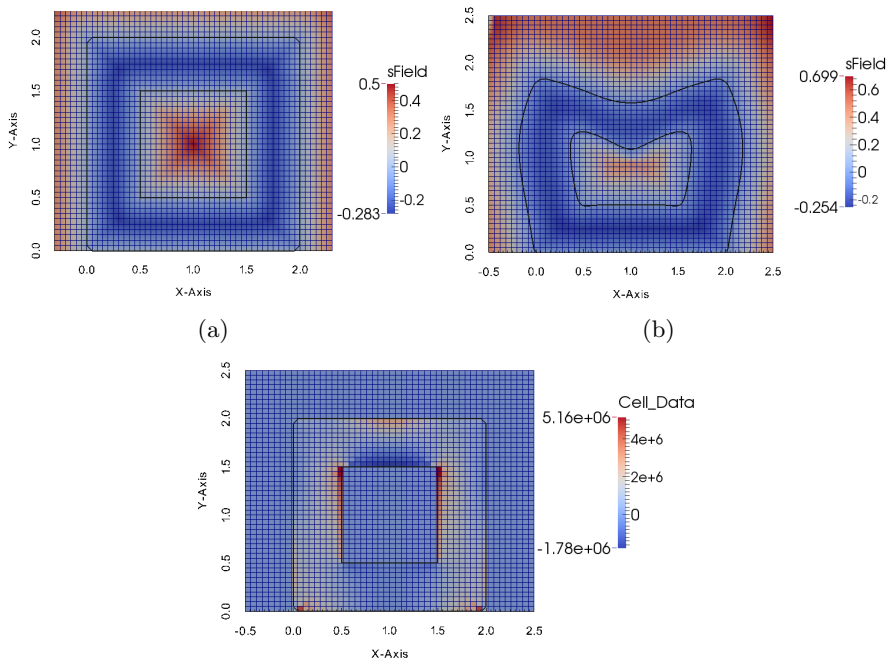

Figure 11: Loaded hollow square. (a) initial configuration, (b) deformed configuration, (c) pressure

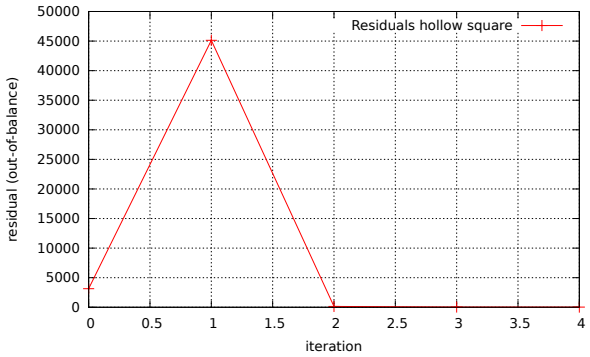

Figure 12: Loaded hollow square. Out-of-balance vector magnitude for one load increment

9 Conclusions

A Fixed Grid Method for Mooney-Rivlin nonlinear material models using the Level Set Method was successfully developed. This method shows to work well for large displacements and large strain problems. It has to be studied how some of the advantages of the Linear Elastic FGFEM may be used, as the matrices computation for the I elements, making this very attractive in the solution of a large amount of problems. Specially, multiphysics problems as Fluid-Structure interaction, nonlinear structural optimization and nonlinear bimaterial problems.

References

[1] Charles Dapogny and Pascal Frey. Computation of the signed distance function to a discrete contour on adapted triangulation. *Calcolo*, 49:193–219, 2012.

[2] Manuel J. Garcia and G. P. Steven. Fixed grid finite elements in elasticity problems. *Engineering Computations*, 16:145–164, 1999.

[3] Seung-Hyun. Ha and Seonho. Cho. Level set based topological shape optimization of geometrically nonlinear structures using unstructured mesh. *Computers and Structures*, 86: 1447â1455, 2008.

[4] Stanley Osher and Ronald Fedkiw. *Level Set Methods and Dynamic Implicit Surfaces*. Springer, 2003.

[5] B. Prabel, A. Combescure, A. Gravouil, and S. Marie. Level set x-fem non-matching meshes: application to dynamic crack propagation in elasticâplastic media. *International Journal for Numerical Methods in Engineering*, 69:1553–1569, 2007.

[6] D.L. Moes N. Sukumar a, N. Chopp and T. Belytschko. Modeling holes and inclusions by level sets in the extended finite-element method. *Computer methods in applied mechanics and engineering*, 190:6183–6200, 2001.

[7] Theodore Sussman and Klauss Bathe. A finite element formulation for nonlinear incompressible elastic and inelastic analysis. *Computers & Structures*, 26:357–409, 1987.

[8] Y. M. Xie and Grant P. Steven. A simple evolutionary procedure for structural optimization. *Computers and Structures*, 49:885–896, 1993.

[9] Hongkai Zhao. A fast sweeping method for eikonal equations. *Mathematics of computation*, 74:603–627, 2004.